Pergamon

Geochimica et Cosmochimica Acta, Vol. 66, No. 14, pp. 2541–2546, 2002
Copyright © 2002 Elsevier Science Inc.
Printed in the USA. All rights reserved
0016-7037/02 $22.00 + .00

PII S0016-7037(02)00846-3

Impurities and nonstoichiometry in the bulk and on the (10$\bar{1}$4) surface of dolomite

KATE WRIGHT,[1,2,*] RANDALL T. CYGAN,[3] and BEN SLATER[2]

[1]Departments of Chemistry and Geological Sciences, University College London, Gower Street, London WCIE 6BT, UK
[2]Royal Institution, 21 Albemarle Street, London W1S 4BS, UK
[3]Geochemistry Department, Sandia National Laboratories, Albuquerque, NM 87185-0750, USA

(*Received July* 13, 2001; *accepted in revised form January* 15, 2002)

Abstract—Atomistic computer simulation methods have been used to model the nature of nonstoichiometry and impurity defects in the bulk and at the (10$\bar{1}$4) surface of dolomite ($MgCa(CO_3)_2$). Calcium and Mg in the bulk and at the surface have been replaced with divalent Ni, Co, Zn, Fe, Mn, and Cd. The results of these calculations indicate that in the bulk, these impurities will prefer to substitute at the Ca site rather than the Mg site. Ca excess in dolomite is most likely incorporated as basal stacking faults; this nonstoichiometry can influence the site distribution of impurities. The calculated surface segregation energies suggest that of all the impurities studied, only Cd will show a strong preference for the (10$\bar{1}$4) surface of dolomite. *Copyright © 2002 Elsevier Science Inc.*

1. INTRODUCTION

Natural dolomites often contain impurities such as Mn, Fe, and other divalent cations that replace either Mg or Ca in the lattice. The site distribution of these impurities is dependent on external factors prevalent at the time of formation, such as temperature, pH, and fluid composition (e.g., Lumsden et al., 1989). In the case of Mn impurities, the degree of nonstoichiometry and disorder is also thought to influence site distribution (Lumsden and Lloyd, 1984). Nonstoichiometry due to Ca enrichment in dolomite is common and characterized by the presence of domains that differ from the ideal ordered dolomite matrix. These domains have been extensively studied by transmission electron microscopy, where they are observed as lamellar-like structural modulations with a wavelength of up to several hundred angstroms (Wenk et al., 1983). The symmetry within these structures is lower than that of dolomite in the surrounding lattice, suggesting that excess Ca is not distributed randomly but concentrated in locally ordered way. A detailed description of Ca excess in dolomites and the models put forward to account for transmission electron microscopic observations can be found in Reeder (1992). In brief, ordered substitution of Ca for Mg may occur on Mg (B) layers only (γ structure) or by the introduction of stacking faults in the basal plane (δ structure). It is not possible, however, to unambiguously identify these structures within dolomite by means of experimental methods.

Ca-rich dolomites are also considered to be more reactive and less stable than those with an ideal Ca:Mg ratio (Reeder, 2000), and thus the presence of Ca excess in dolomite may be a factor in determining the site distribution and concentration of impurities. Understanding such relations, and the way in which dolomite surfaces interact with impurities, could provide clues to the conditions of formation of dolomite in the geological past. Although surface complexation models have been developed to study Mg and Ca complexing on dolomite surfaces (e.g., Brady et al., 1996; Pokrovsky et al., 1999), no systematic studies have been carried out to determine surface speciation associated with impurities. Therefore, the aim of this study is to investigate the site partitioning of impurities in the bulk dolomite lattice and on the common (10$\bar{1}$4) surface via atomistic simulation techniques. The energetics of the different Ca excess structures and their effects on impurity substitution are also evaluated.

* Author to whom correspondence should be addressed (kate@ri.ac.uk).

2. COMPUTATIONAL METHODS

Computer simulation techniques have been widely and successfully used to study both the perfect and defective lattice properties of a range of geologically important minerals (e.g., Wright and Jackson, 1995; Wright et al., 1996; Sokol et al., 1998). The atomistic simulation method is based on the Born model of solids where interatomic potential functions are defined to model the long- and short-range forces acting between atoms or ions in the solid. The effects of oxygen ion polarizability on the system are included by use of the shell model (Dick and Overhauser, 1958), whereas directionality of the bonding is described by three-body and four-body terms. The variable potential parameters are derived by fitting to experimental data such as structure, elastic constants, and vibrational spectra. Simulations are carried out by means of standard energy minimization schemes in which the energy of the system is calculated with respect to all atomic coordinates. Thus, the equilibrium positions of the ions are evaluated by minimizing the lattice energy until all forces acting on the crystal are removed.

In ionic and semi-ionic materials, defects are charged species and cause long-range disruption in the crystal lattice. These long-range perturbations can be effectively modeled by means of the approach developed by Mott and Littleton (1938), where the crystal is divided into two concentric spherical regions, R1 and R2, as illustrated in Figure 1a. In R1, which contains the defect at its center, an explicit simulation is carried out to adjust the coordinates of all ions in the region until they are at positions where no forces are acting on them—that is, they are relaxed around the defect. The radius of R2 is selected so that the forces within this super sphere are relatively weak and the relaxation can be treated essentially as the polarization response to the effective charge of the defect. An interfacial region (R2A) is introduced to deal with interactions between the two regions. The resulting defect energy is then a measure of the perturbation by the defect on the static lattice energy of the crystal. In this approach, both the zero point energy and the effects of entropy are neglected. However, it has the advantage that single charged defects or small defect clusters can be considered in isolation so as to mimic infinitely dilute concentrations.

An alternative approach is to use a supercell (SC) method where the defect is part of a periodic three-dimensional repeat unit (Fig. 1b). If single defects or low defect concentrations are to be considered, then

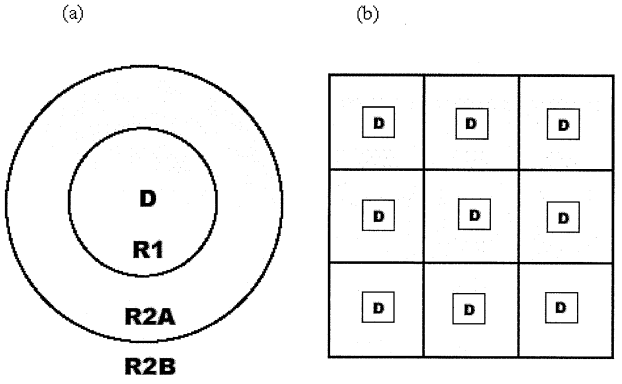

Fig. 1. Representation of the ML (a) and SC (b) methods for the calculation of defect energies. In the ML method (a), a single defect, D, is at the center of R1. In Figure 1b, the defect cell is periodically repeated.

the SC must be sufficiently large so as to minimize defect–defect interactions. In practice, it is often prohibitively expensive in terms of computational resources to use the SC method, and where defect–defect interactions are important, the Mott-Littleton (ML) method is more appropriate. However, where high concentrations of defects interacting in a periodic way are to be modeled, then the SC method is more applicable. The advantage of the SC method is that algorithms for the calculation of free energies can be used, thus including the effects of entropy on the defect energy. In addition, the influence of defects on cell volume can be assessed.

For the calculation of surface structures, the most commonly used approach is to treat the crystal as planes of atoms that are periodic in two dimensions. Surfaces are modeled by considering a single block; two blocks together simulate the bulk, or a more complex interface. The simulation block is divided into two regions similar to that described for bulk defects above. The near-surface region, R1, is composed of those atoms adjacent to the surface or interface, and an outer region, R2. The atoms in R1 are allowed to relax to their minimum energy configuration, whereas the ions of R2 are held fixed at their bulk equilibrium positions. The specific surface energy is defined as the energy per unit area required to form the crystal surface relative to the bulk. The surface energy (γ) is therefore given by

$$\gamma = \frac{U_s - U_b}{A} \quad (1)$$

where U_s refers to the energy of region 1 for the surface, U_b refers to the energy of an equivalent number of bulk atoms, and A is the surface area. The lower the surface energy, the more stable the surface will be, and the more prevalent one would expect that face to be in the crystal habit.

The effects of changing the surface stoichiometry on surface energy and stability can also be considered by substitution of impurity ions for Ca and Mg, and by changing the Ca:Mg ratio in the surface layer. This then allows us to calculate the segregation energy of a particular ion between the surface and an aqueous fluid. The segregation energy is defined as the energy required to exchange a cation in the surface layer with an impurity in solution. If the resulting energy is negative, then the reaction is favored; if it is positive, then the impurity will stay in solution. The segregation energy is calculated in two steps (Titiloye et al., 1998). First, we calculate the energy required to remove an ion from the surface and replace it with an impurity:

$$M1_{surf} + M2_{(g)} \Rightarrow M1_{(g)} + M2_{surf} \quad (2)$$

where M1 is Ca or Mg and M2 is the impurity, and the energy for this reaction is obtained directly form the simulation. The second step involves the dehydration of the impurity and corresponding hydration of the ion removed from the surface:

Table 1. Comparison of impurity substitution energies (eV) at Ca and Mg sites in dolomite as calculated by the Mott-Littleton (ML) and supercell (SC methods).

Substitution at impurity	Ca sites		Mg sites	
	ML	SC	ML	SC
Ni	−3.07	−3.34	−0.73	−0.73
Co	−2.54	−2.56	−0.11	−0.14
Fe	−2.38	−2.36	0.24	0.21
Zn	−2.51	−2.53	−0.07	−0.11
Mn	−1.86	−1.96	0.90	0.85
Cd	−1.17	−1.18	1.96	1.85

$$M1_{(g)} + M2_{(aq)} \Rightarrow M1_{(aq)} + M2_{(g)} \quad (3)$$

where values for these parameters have been obtained form standard thermodynamic tables (De Lide, 1994).

In the present study, we use the interatomic potential set of Fisler et al. (2000), which was derived to model a range of metal carbonate minerals. These potentials have been successfully used to simulate the bulk properties (Fisler et al., 2000) and surface structure (Wright et al., 2001) of calcite, magnesite, and dolomite. For the simulation of bulk defects, we have used the General Utility Lattice Program (GULP) of Gale (1997), which is able to implement both the ML and SC defect methodologies. For the former approach, a R1 size of 10 Å containing 314 ions and R2 of 21.5 Å was found to be sufficient to converge defect energies in these systems. In the case of the SC calculations, the simulation temperature was set to 300 K and either a $2 \times 2 \times 1$ or $1 \times 1 \times 2$ SC used. For the study of surface defects, we have used the 2D code MARVIN (Gay and Rohl, 1995), with a repeating slab containing 300 ions and having a surface area of 233 Å^2. This configuration, with five layers R1 and seven in R2, was found to be the optimum required to accommodate full surface relaxation (Wright et al., 2001).

3. RESULTS AND DISCUSSION

3.1. Bulk Defects

Intrinsic and extrinsic defect energies in dolomite were first calculated by means of the ML method described above; then, free energy calculations were performed at 300 K. The effects of increasing SC size were investigated by comparing the formation energy of a simple Ca_{Mg} substitution at 0 K with that of the corresponding ML energy. For a SC of $19.2 \times 19.2 \times 16.1$ Å ($4 \times 4 \times 1$ U cells) containing 480 ions, the formation energy is 3.32 eV, which compares with 3.34 eV from the ML and gives a defect–defect interaction energy of −0.03 eV. For the smaller SCs used in the calculations of $2 \times 2 \times 1$ and $1 \times 1 \times 2$ U cells, the defect–defect interaction energies are −0.04 eV for both cells. Thus, eliminating defect–defect interactions entirely would require a prohibitively large SC.

Substitution energies for the impurities Fe^{2+}, Co^{2+}, Mn^{2+}, Zn^{2+}, Ni^{2+}, and Cd^{2+} at Ca^{2+} and Mg^{2+} sites were calculated by means of both ML and SC methods and are listed in Table 1. The results obtained by the ML methods give energies for truly isolated defects, whereas those from the SC calculations represent a composition $[M1_{0.916}M2_{0.084}M3_{1.0}](CO_3)_2$, where M2 is the impurity that substitutes on an M1 site but not on an M3 site and M1 can be Ca or Mg. Both methods show similar energies, and in all cases, substitutions are favored on Ca rather than Mg sites. Figure 2 shows the substitution energies calculated via the ML method, plotted as a function of ionic radius. For substitutions on both Ca and Mg sites, the calculated

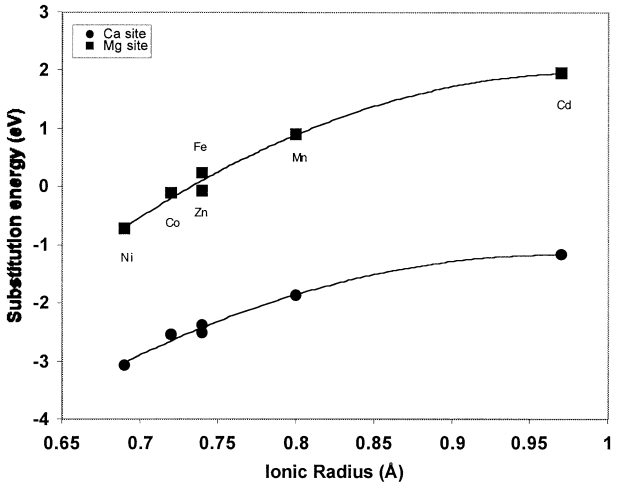

Fig. 2. Impurity substitution energies at Mg and Ca sites in dolomite as a function of ionic radius calculated by the ML method.

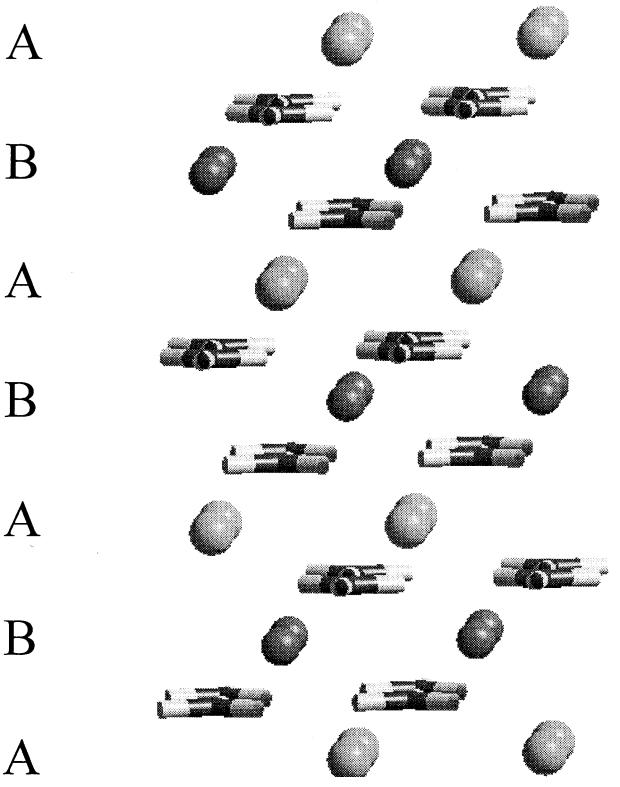

Fig. 3. The dolomite unit used in the simulation of the γ and δ Ca excess structures where A layers contain Ca ions and B Mg ions. For the γ structure, two of the four Mg ions on every B layer were replaced by Ca, and for the δ structure, all Mg on a B layer was replaced. The unit was embedded in a perfect dolomite lattice for the ML calculations, but for the SC calculations, a larger cell was used as a periodic repeat unit.

energies increase with increasing ionic radius, where Ni is the most favorable defect and Cd the least favorable. This trend is not unexpected and is the same as that found by Fisler et al. (2000) for calcite. The difference between the substitution energies at the two sites is not constant with increasing radii but increases slowly from 2.34 eV for Ni to 3.13 eV for Cd. Analysis of the different components of the defect energy show that it is dominated by the Coulombic term; thus, the effect of the defect on the lattice is predominantly electrostatic. Analysis of local structure around the defect shows that nearest neighbor M-O distances vary depending on the difference in ionic radii between impurity and Ca or Mg. In the bulk, M-O distances are 2.10 Å (Mg-O) and 2.39 Å (Ca-O), whereas for Ni_{Ca}, the distance reduces to 2.18 Å, and for Cd_{Mg}, it increases to 2.26 Å. Distortion around the defect site is minimal and does not extend past the nearest neighbor carbonate groups so that there is little or no medium- to long-range strain on the lattice.

To investigate the way in which dolomite may accommodate excess Ca and ordering on the Ca (A) and Mg (B) sublattices, we have simulated a range of Ca/Mg substitution schemes that relate to the δ and γ structures outlined in the Introduction. With the ML method, the γ structure is obtained by creating a defective unit consisting of six cation layers where half of the sites in each Mg (B) layer are replaced by Ca in an ordered fashion (Fig. 3). This configuration represents a small, Ca-rich unit in an otherwise perfect dolomite lattice. Creation of the δ structure involves the formation of a stacking fault and is modeled by replacing all Mg ions in a B layer by Ca. Once again, the Ca-rich block is represented by a six-cation layer unit surrounded by perfectly ordered dolomite. The energies per Ca_{Mg} substitution for the γ and δ configurations are 3.38 and 3.26 eV, respectively. Of course, in real dolomites, the modulated structures observed via transmission electron microscopy are much more extensive than those described above, which have only four cations in each of the six layers. Therefore, we have performed calculations using SCs in which the whole system is defective. For the γ structure, we use the $2 \times 2 \times 1$ SC; for the δ structure, we use a $1 \times 1 \times 2$ SC.

The results of these calculations are presented in Table 2 and show that incorporation of Ca as stacking faults—that is, the δ structure has a slightly lower energy than ordered Ca_{Mg} substitution on B layers (γ structure). The same result is given by both the ML and the SC methods, and thus the infinite limit and high limit are in complete agreement, although it should be noted that the energy differences are small. The Mg/Ca exchange energy is similar for the isolated defects and the γ structure and more than double that calculated for the δ structure. Calorimetric experiments by Navrotsky et al. (1999) have

Table 2. Calculated intrinsic defect formation energies (eV per defect) in dolomite.

Defect	ML	SC
V_{Ca}	19.76	
V_{Mg}	23.61	
Ca_{Mg}	3.34	
Mg_{Ca}	−2.45	
Mg/Ca exchange δ disorder	0.90	
Ca_{Mg}	3.26	3.06
Mg_{Ca}	−2.69	−2.65
Mg/Ca exchange γ disorder	0.37	0.33
Ca_{Mg}	3.38	3.18
Mg_{Ca}	−2.54	−2.43
Mg/Ca exchange	0.84	0.79

Table 3. Mean field energies (eV) for partial occupancy of a single Ca and Mg site by Mn.

Mn mean occupancy			
Mg site	Ca site	Stoichometric	Ca rich
0.02	0.98	−1.78	−2.10
0.20	0.80	−1.22	−1.55
0.80	0.20	0.42	0.03
0.98	0.02	0.85	0.47

suggested that the enthalpy of disordering for dolomite is in the region of 35 kJmol^{-1}, which is in excellent agreement with the calculated Mg/Ca exchange energy of 0.37 eV (35.7 kJmol^{-1}) for the δ structure.

Unlike calcite, experimental studies of impurity substitution in dolomite are few and mainly relate to Fe and Mn. For Fe, it is generally assumed that Fe will substitute at the Mg site because the two have a similar ionic radius. Ankerite, the Fe rich variety of dolomite, commonly occurs as a Ca-rich phase. Studies of the site partitioning of Mn between Ca and Mg sites have been carried out using cathodoluminescence and electron paramagnetic resonance techniques (see Galoisy, 1996, and references therein). The findings from cathodoluminescence and electron paramagnetic resonance suggest that Mn has a definite preference for the Mg site. However, it seems likely that other defects and impurities in the structure can influence the site preference, as can growth kinetics (Angus et al., 1984). The calculations predict a strong preference of all impurities for the Ca site, at variance with the available experimental findings that suggest other factors that we have not considered are having an influence.

The potential parameters were derived in a self-consistent manner to be applicable to a range of carbonate phases and have been well tested (Fisler et al., 2000). An alternative way to calculate defect energetics is to use electronic structure methods. Therefore, preliminary calculations were carried out by the periodic CASTEP code version 4.2 (licensed under UKCP-MSI 1999; Payne et al., 1992), which uses a plane wave and pseudopotential description of nuclei and electrons in the system within the framework of density functional theory (Payne et al., 1992). These calculations give values of −3.34 and 1.10 eV for Mn substitution at Ca and Mg sites, respectively, where Mn is in a low-spin state. For Mn in a high-spin configuration, the substitution energy at the Ca and Mg sites are, respectively, −3.38 and 1.20 eV. These energies are higher than those obtained via the atomistic techniques but do show the same Ca site preference and therefore suggests that the use of these potentials to calculate substitution energies is valid. In addition, we have carried out a series of mean field calculations within GULP, where one or more of the metal sites experiences a potential that is the mean of that of Mg or Ca, and Mn. Different occupancies of Mn at Mg sites have been calculated for both stoichiometric and Ca-rich dolomite; the results are listed in Table 3. Note that the occupancies were chosen to be comparable with the distributions found from experiment. For high Mn_{Ca} occupancies—that is, low Mn_{Mg} occupancy—the energies are still more favorable than for high Mn_{Mg} occupancy, even when excess Ca is present. These calculations were also performed for Fe occupancies; the results are similar to those found for Mn. This leads to the conclusion that some other factor, one not considered in our model, is responsible for lowering the energy of substitution at Mg sites.

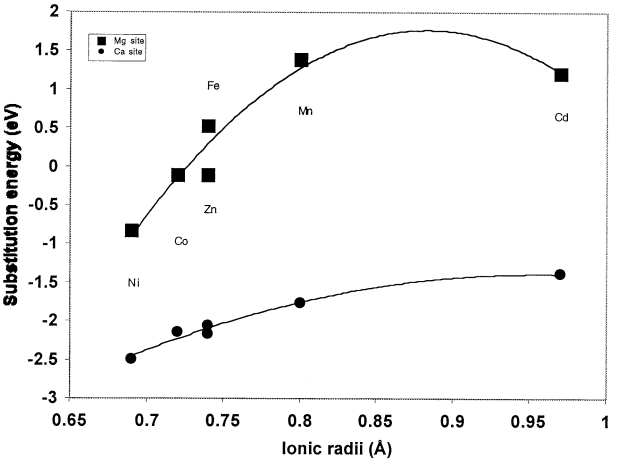

Fig. 4. Impurity substitution energies on the hydrated (10$\bar{1}$4) surface of dolomite as a function of ionic radius.

One possible explanation for the favorable energy of the Mg-site substitution is that substitution may occur at Ca excess sites (i.e., Mg sites already substituted by Ca). We have already seen that Mn substitution energies in the mean field calculations are lowered if excess Ca is present. For Ca replacing Mg along a stacking fault, the substitution energy is 3.06 eV; for Mn_{Mg} substitution, the energy is 0.85 eV. Thus, if Mn replaces Ca at an Mg site the energy saving is 0.85 to 3.06 = −2.21 eV, which is 0.25 eV more favorable than the Mn_{Ca} substitution. This trend is observed for all of the impurity cations considered in this work, suggesting that the dominant mechanism for such a solid-state reaction is enthalpic rather than kinetic. This type of reaction will not be important when considering incorporation of impurities during crystal growth.

3.2. Surface Defects and Segregation

For consideration of surface defects, Ca and Mg in the (10$\bar{1}$4) surface layer were replaced by each of the six impurity ions in turn. In all cases, the surface was solvated by a monolayer of water that had been relaxed to its minimum energy configuration (Wright et al., 2001). Figure 4 shows the energetics of substitution with ionic radius, and as can be seen, the general trend observed for bulk substitutions is followed at the surface as well—that is, that Ca is more likely to exchange with impurity cations at the surface than Mg.

By use of the values obtained for surface substitution and standard thermodynamic data for each metal ion in the gas and aqueous phase (De Lide, 1994), the segregation energies can be calculated to show if a particular ion will stay in solution or exchange with a surface cation. The values obtained are given in Table 4 where a negative segregation energy indicates a preference for the surface and a positive one, a preference for the fluid. Of all the cations considered, Cd is the only one that prefers to be in the surface rather than remain in solution and will segregate most strongly to the Mg surface site. This is the opposite of that indicated by substitution energies alone and

Table 4. Surface segregation energies ($kJmol^{-1}$) in dolomite with respect to hydrated ions in aqueous solution. An ion with a negative segregation energy will prefer to exchange with a surface ion. No data were available for Co in aqueous solution.

	Segregation energy	
Impurity	Ca site	Mg site
Mg	151.48	0.00
Ni	277.88	160.17
Co		
Zn	259.55	109.99
Fe	174.64	78.15
Mn	422.61	380.16
Cd	−8.68	−86.84
Ca	0.00	−22.19

can be accounted for by the differing hydration energies of Ca and Mg, which are −542.8 and 466.9 $kJmol^{-1}$, respectively (De Lide, 1994). One can also consider a more complex mechanism for incorporation of impurities at the surface such as substitution on a surface where there is Ca or Mg excess. In this case, substitution would occur at a Ca_{Mg} or Mg_{Ca} site. However, the segregation energies for such reactions show a similar trend to those for direct substitution and once again only Cd is predicted to exchange.

There are differences, however, between substitution trends at the surface and in the bulk. Comparison of Figures 2 and 4 shows that for substitution at the Ca site, the slope of the energy vs. ionic radius curve is very similar, although it has been shifted up in scale (i.e., the energies are less favorable) for the surface relative to the bulk. It is possible, therefore, that substitution at this site will become less favored as the coordination number of Ca decreases. The situation is less clear when considering substitution at the Mg site, where the gradient of the curve is much steeper for the surface than for the bulk. As coordination decreases, the Mg site seems to become more sensitive to the ionic radius of the substituting ion, so that the larger cations are less favored .

Incorporation of impurities into dolomite during growth will be influenced by the availability of sorption sites at the surface. In this study, we have considered impurity substitution on flat terraces only where only two cation sites are present. On real surfaces, the existence of growth steps and kinks at the surface will increase the number of distinctly different sites that can sorb or exchange impurity cations, and each will do so with a different energy. No data are available on impurity substitution on dolomite or on magnesite, although a substantial body of literature exists on impurities in calcite. On the $(10\bar{1}4)$ surface of calcite, the divalent cations Co, Cd, and Zn preferentially sorb at structurally distinct sites so that during coprecipitation experiments, nonequivalent step growth rates are observed (Reeder, 1996). This site dependence is also thought to be partly responsible for the difference between the measured calcite-solution distribution coefficients of impurities and those predicted by thermodynamic relationships (Rimstidt et al., 1998) and provides a mechanism for the trapping of impurities on particular sites in the bulk structure. The preference shown in this study for Cd surface exchange on dolomite suggests that it is more easily incorporated into the five-coordinate sites on flat terraces than the other cations considered. The incorporation of impurities into dolomite during growth will also be influenced by factors such as fluid composition and pH, although it appears that excess Ca at the surface will inhibit exchange with ions in solution. Although our calculations deal only with cation exchange on the defect free $(10\bar{1}4)$ surface, they can provide useful information on the broad trends that can be expected. It is more likely, however, that impurity substitutions will occur at high index surfaces where low coordinated surface cations are present. Such surfaces tend to have larger surface energies that can be a factor in enhancing growth, especially for small grain sizes. Impurities could then become trapped at particular, low coordination sites during growth that reflect the relative solution kinetics of the surface cations.

4. CONCLUSIONS

The results of the bulk defect simulations presented in the previous section indicate a strong preference of impurity elements for Ca rather than Mg sites in dolomite, with substitution energy increasing with increasing ionic radii. This trend is predicted for substitution at both bulk and surface sites, although in the case of $(10\bar{1}4)$ surface substitution, the segregation energy can be a more useful indicator of reactivity. In the case of Ca excess in the bulk crystal, our calculations show that such substitutions will occur in an ordered fashion, most likely as basal stacking faults. Ca-rich dolomites are shown to favor bulk impurity substitution at Mg sites, although when the excess is present at the surface, cation exchange with aqueous ions is inhibited. For stoichiometric surfaces, Cd is the most easily incorporated impurity ion for the surface substitutions involving direct exchange with Mg. Future work in this area will investigate the interaction of impurities with other dolomite surfaces, as well as with surface defects, particularly kink and step sites and high index faces.

Acknowledgments—We thank Dr. Pat Brady for useful discussion during the early stages of this manuscript and to R. Reeder and an anonymous referee for comments. K.W. thanks the Royal Society for support under their University Research Fellowship scheme. R.T.C. is grateful for the funding provided by the U.S. Department of Energy, Office of Basic Energy Sciences, Geosciences Research, under contract DE-AC04-94AL85000 with Sandia National Laboratories.

Associate editor: G. Sposito

REFERENCES

Angus J. C., Beveridge B., and Raynor B. J. (1984) Dolomite thermometry by electron spin resonance (ESR). *Chem. Geol.* **43,** 331–346.

Brady P. V., Krumhansl J. L., and Papenguth H. W. (1996) Surface complexation clues to dolomite growth. *Geochim. Cosmochim. Acta* **60,** 727–731.

CRC Handbook of Chemistry and Physics (ed. D. R. De Lide). 75th ed 1994. CRC Press.

CASTEP4.2 Academic Version licensed under the UKCP-MSI agreement 1999.

Dick B. G. and Overhauser A. W. (1958) Theory of the dielectric constants of alkali halide crystals. *Phys. Rev.* **112,** 90–103.

Fisler D. K., Gale J. D., and Cygan R. T. (2000) A shell model for the simulation of rhombohedral carbonate minerals and their point defects. *Am. Mineral.* **85,** 217–224.

Gale J. D. (1997) GULP: A computer program for the symmetry adapted simulation of solids. *J. Chem. Soc. Faraday Trans.* **93,** 629–637.

Galoisy L. (1996) Local versus average structure around cations in minerals from spectroscopic and diffraction measurements. *Phys. Chem. Minerals* **23,** 217–225.

Gay D. H. and Rohl A. L. (1995) MARVIN: A new computer code for studying surfaces and interfaces and its application to calculating the crystal morphologies of corundum and zircon. *J. Chem. Soc. Faraday Trans.* **91,** 925–936.

Lumsden D. N. and Lloyd R. V. (1984) Mn (II) partitioning between calcium and magnesium sites in studies of dolomite origin. *Geochim. Cosmochim. Acta* **48,** 1861–1865.

Lumsden D. N., Shipe L. G., and Lloyd R. V (1989) Mineralogy and Mn geochemistry of laboratory synthesized dolomite. *Geochim. Cosmochim. Acta* **53,** 2325–2329.

Mott N. F. and Littleton M. J. (1938) Conduction in polar crystals. I Electrolytic conduction in solid salts. *J. Chem. Soc. Faraday Trans.* **34 ,** 485–499.

Navrotsky A., Dooley D., Reeder R., and Brady P. (1999) Calorimetric studies of the energetics of order-disorder in the system $(Mg_{1-x}Fe_xCa(CO_3)_2$. *Am. Mineral.* **84,** 1622–1626.

Payne M. C., Teter M. P., Allan D. C., Arias T. A., and Joannopoulos (1992) Iterative minimization techniques for ab initio total-energy calculations: Molecular dynamics and conjugate gradients. *Rev. Mod. Phys.* **64,** 1045–1097.

Pokrovsky O. S., Schott J., and Thomas F. (1999) Dolomite surface speciation and reactivity in aquatic systems. *Geochim. Cosmochim. Acta* **63 ,** 3133–3143.

Reeder R. J. (1992) Carbonates: Growth and alteration microstructures. *Rev. Mineral.* **27,** 381–424.

Reeder R. J. (1996) Interaction of divalent cobalt, zinc, cadmium and barium with the calcite surface during layer growth. *Geochim. Cosmochim. Acta* **60,** 1543–1552.

Reeder R. J. (2000) Constraints on cation order in calcium-rich sedimentary dolomite. *Aquat. Geochem.* **6,** 213–226.

Rimstidt J. D., Balog A., and Webb J. (1998) Distribution of trace elements between carbonate minerals and aqueous solutions. *Geochim. Cosmochim. Acta* **62,** 1851–1863.

Sokol A. A., Catlow C. R. A., Garces J. M., and Kuperman A. (1998) Defect centres in microporous aluminum silicate materials. *J. Phys. Chem.* **102,** 10647–10649.

Titiloye J. O., de Leeuw N. H., and Parker S. C. (1998) Atomistic simulation of the differences between calcite and dolomite surfaces. *Geochim. Cosmochim. Acta* **62,** 2637–2641.

Wenk H.-R., Barber D. J., and Reeder R. J. (1983) Microstructures in carbonates. *Rev. Mineralogy.* **11,** 301–367.

Wright K. and Jackson R. A. (1995) Computer simulation of the structure and defect properties of zinc sulphide. *J. Mater. Chem.* **5,** 2037–2040.

Wright K., Catlow C. R. A, and Freer R. (1996) Water related defects and oxygen diffusion in albite. *Contrib. Miner. Petrol.* **125,** 161–166.

Wright K., Cygan R. T., and Slater B. (2001) Structure of the $(10\bar{1}4)$ surfaces of calcite, dolomite and magnesite under wet and dry conditions. *Phys. Chem. Chem. Phys.* **3,** 839–844.